STEM CELLS®

TRANSLATIONAL AND CLINICAL RESEARCH

Dedifferentiation-Reprogrammed Mesenchymal Stem Cells with Improved Therapeutic Potential

YANG LIU,[a,b]* XIAOHUA JIANG,[a,c]* XIAOHU ZHANG,[a]* RUI CHEN,[a] TINGTING SUN,[a] KIN LAM FOK,[a] JIANDA DONG,[a] LAI LING TSANG,[a] SHAOQIONG YI,[d] YECHUN RUAN,[a] JINGHUI GUO,[a] MEI KUEN YU,[a] YUEMIN TIAN,[a] YIU WA CHUNG,[a] MO YANG,[e] WENMING XU,[a,f] CHIN MAN CHUNG,[a] TINGYU LI,[b†] HSIAO CHANG CHAN[a,c,f†]

[a]Epithelial Cell Biology Research Center, School of Biomedical Sciences, Faculty of Medicine, Chinese University of Hong Kong, Shatin, Hong Kong; [b]Children's Hospital, Chongqing Medical University, Chongqing, People's Republic of China; [c]Key Laboratory for Regenerative Medicine of Ministry of Education, Jinan University-the Chinese University of Hong Kong, Guangzhou, People's Republic of China; [d]Department of Applied Molecular Biology, Institute of Microbiology and Epidemiology, Academy of Military Medical Sciences, Beijing, People's Republic of China; [e]Department of Hematology, Nanfang Hospital, Southern Medical University, Guangzhou, People's Republic of China; [f]Sichuan University–the Chinese University of Hong Kong Joint Laboratory for Reproductive Medicine, Key Laboratory of Obstetric, Gynecologic and Pediatric Diseases and Birth Defects of Ministry of Education, West China Women's and Children's Hospital, Sichuan University, Chengdu, People's Republic of China

Key Words. Dedifferentiation • Reprogramming • miRNA-34a • Enhanced survival • Mesenchymal stem cells

ABSTRACT

Stem cell transplantation has been shown to improve functional outcome in degenerative and ischemic disorders. However, low in vivo survival and differentiation potential of the transplanted cells limits their overall effectiveness and thus clinical usage. Here we show that, after in vitro induction of neuronal differentiation and dedifferentiation, on withdrawal of extrinsic factors, mesenchymal stem cells (MSCs) derived from bone marrow, which have already committed to neuronal lineage, revert to a primitive cell population (dedifferentiated MSCs) retaining stem cell characteristics but exhibiting a reprogrammed phenotype distinct from their original counterparts. Of therapeutic interest, the dedifferentiated MSCs exhibited enhanced cell survival and higher efficacy in neuronal differentiation compared to unmanipulated MSCs both in vitro and in vivo, with significantly improved cognition function in a neonatal hypoxic–ischemic brain damage rat model. Increased expression of *bcl-2* family proteins and microRNA-34a appears to be the important mechanism giving rise to this previously undefined stem cell population that may provide a novel treatment strategy with improved therapeutic efficacy. STEM CELLS *2011;29:2077–2089*

Disclosure of potential conflicts of interest is found at the end of this article.

INTRODUCTION

Bone marrow stromal stem cells, also known as mesenchymal stem cells (MSCs), were initially identified as a population of organized hierarchical adult stem cells with the potential to differentiate into mesodermal lineage cells such as osteocytes, chondrocytes, and adipocytes [1, 2]. However, recent studies have demonstrated the pluripotency of MSCs in that they have the ability to cross oligolineage boundaries which were previously thought to be impenetrable [3–6] and be induced to differentiate into various kinds of cell types, such as

Author contributions: Y.L. and X.Z.: collection and/or assembly of data, data analysis and interpretation, manuscript writing, and final approval of manuscript; X.J.: design, collection and/or assembly of data, data analysis and interpretation, manuscript writing, and final approval of manuscript; R.C., T.S., K.L.F., J.D., L.L.T., S.Y., Y.R., J.G., M.K.Y., Y.T., and W.X.: collection and/or assembly of data, data analysis and interpretation, and final approval of manuscript; Y.W.C.: collection and/or assembly of data, data analysis and interpretation, administrative support, and final approval of manuscript; M.Y.: data analysis and interpretation, provision of study material, and final approval of manuscript; C.M.C.: collection and/or assembly of data and data analysis and interpretation, T.L.: conception and design, financial support, provision of study material, data analysis and interpretation, and final approval of manuscript; H.C.C: conception and design, financial support, provision of study material, data analysis and interpretation, manuscript writing, and final approval of manuscript.

*Contributed equally as first authors.

†Contributed equally as corresponding authors.

Correspondence: Hsiao Chang Chan, Ph.D., Epithelial Cell Biology Research Center, School of Biomedical Sciences, Faculty of Medicine, the Chinese University of Hong Kong, Shatin, Hong Kong. Telephone: 852-26961105; Fax: 852-26037155; e-mail: hsiaocchan@cuhk.edu.hk; or Tingyu Li, M.D., Children's Hospital, Chongqing Medical University, Chongqing, China. Telephone: 8623-63628660; Fax: 8623-63626904; e-mail: tyli@vip.sina.com Received January 25, 2011; accepted for publication September 27, 2011; first published online in STEM CELLS *EXPRESS* November 3, 2011. 1066-5099/2011/$30.00/0 doi: 10.1002/stem.764

cardiomyocytes [7–9], hepatocytes [10, 11], and endothelial cells [12]. Especially, a large of body of evidence have indicated that mouse, rat, and human bone marrow MSCs can be induced to differentiate to neuron-like cells in culture [13–16] and further verified by the transplantation experiments in animal models of Parkinson's disease [17], stroke [18, 19], cerebral ischemia [20], spinal cord injury [21], and Niemann-Pick disease [22]. However, despite many transplantation studies showing beneficial effects, most studies report low levels of cell persistence and neuronal differentiation in vivo. In particular, when MSCs are injected directly into the lesion tissues, massive death of transplanted cells has been observed [20, 23, 24]. This greatly limits their overall effectiveness and clinical use.

Dedifferentiation has been considered as one of the mechanisms rerouting cell fate by reverting differentiated cells to an earlier, more primitive phenotype characterized by alterations in gene expression pattern which confer an extended differentiation potential [25]. In urodele amphibians, cell dedifferentiation is a common mechanism resulting in the functional regeneration of complex body structures throughout life [26, 27]. In mammals, the differentiation process is normally irreversible in differentiated cells [28]. However, recent studies have provided evidence that terminally differentiated mammalian cells can undergo dedifferentiation on injury [29, 30] or when the cells are cultured under special conditions [30–34]. Previous studies from both our group and others have demonstrated that on withdrawal of extrinsic stimulation, MSC-derived neurons are able to revert back to MSC morphologically [35, 36]. However, the question as to whether the dedifferentiated MSCs (De-MSCs) are identical to or different from their original counterparts has not been addressed and their therapeutic potential is not explored. In this work, we set out to address these questions by using monoclonal MSCs. For the first time, we have identified a population of De-MSCs with a variety of genetic and phenotypic characteristics distinct from their original counterparts. Of therapeutic interest, the De-MSCs exhibited enhanced cell survival and higher efficacy in neuronal differentiation compared to unmanipulated MSCs both in vitro and in a neonatal hypoxic–ischemic brain damage (HIBD) rat model in vivo (see graphic abstract in Supporting Information Fig. S1). This study has also revealed possible mechanisms involving bcl-2 family proteins and miR-34a in the reprogramming process.

Materials and Methods

MSCs and Induction of Differentiation, Dedifferentiation, and Redifferentiation

Rat bone marrow MSCs were isolated and expanded as previously described [13]. To obtain monoclonal MSCs, cells were diluted in 10 cells per milliliter and then seeded in 96-well plate. Four individual MSC clones were established and exhibited similar characteristic MSC phenotype as detected by surface markers. MSCs of passage 8–25 were grown on either poly-L-lysine-coated cover slips in six-well plate (2×10^4 per well) or 75-cm^2 plastic flask (5×10^5) in Dulbecco's modified Eagle medium (DMEM)/F12/10% fetal bovine serum (FBS) for 24 hours, and the media were then replaced with preinduction media consisting of DMEM/F12/10% FBS/10^{-7} M all-*trans*-retinoic acid (ATRA) and 10 ng/ml basic fibroblast growth factor (bFGF). To initiate neuronal differentiation, the cells were washed with phosphate-buffered saline (PBS) and then transferred to neuronal induction media composed of modified neuronal medium (MNM, DMEM/2% dimethyl sulfoxide/200 μM butylated hydroxyanisole/25 mM potassium chloride/2 mM valproic acid/10 μM forskolin/1 μM hydrocortisone/5 μg/ml insulin) for 24–48 hours. In another set of experiment, the cells were collected at 2, 8, 24, 48, and 72 hours after neuronal induction for further characterization. After neuronal induction, MNM was replaced with DMEM/F12 containing 10% FBS. Cells resumed stem cell characteristics 24 hours later and were allowed to grow for another 24 hours. These cells were considered De-MSCs at passage 1. Subsequently, the De-MSCs were passaged every 4–5 days when they reached 80% confluence. To induce neuronal redifferentiation, the full media were removed, the cells were washed with PBS, and transferred to MNM again [36]. Green fluorescent protein (GFP) MSCs were obtained from 6-week-old GFP-transgenic Sprague-Dawley (SD) rats ("green rat CZ-004" SD TgN [CAG–enhanced GFP] OsbCZ-004). Primary hippocampal neurons (PHNs) were isolated from the hippocampus of 1-day-old SD rat, as previously described [37].

Animal Studies

In vivo studies were performed with the approval of the Animal Experimentation Ethics Committee of the Chinese University of Hong Kong. Neonatal HIBD model was established as described before [38]. Briefly, the right common carotid artery of 7-day postnatal SD male rat pups was permanently doubly ligated. After 2-hour recovery, the pups were subjected to a humidified mixture of 8% O_2 and 92% N_2 at 37°C for another 2 hours. After 5 days of hypoxia–ischemia, the pups were randomly divided into three groups and infused with 1–2 $\times$ 10^5 MSCs or De-MSCs in 5 μL of PBS into the right lateral cerebral ventricle. Shuttle box test, as illustrated in Supporting Information Fig. S11, was performed as described before [39] to evaluate the ability of learning and memory in six continuous sessions for 6 days, and the seventh and eighth sessions were followed 1 and 2 months later, respectively. In another set of experiments, 3 or 7 days after transplantation, the animals were sacrificed and the tissues were prepared for immunohistochemistry staining to further evaluate the efficacy of graft and differentiation.

Results

Dedifferentiation of MSC-Derived Neuronal Progenitors

Clonally derived MSCs displayed the characteristic spindle shape or flat polygonal morphology (Fig. 1AA′, Supporting Information Fig. S2aa′) and their phenotypic traits remained relatively stable with increasing number of passages. Immunodetection of a set of cell surface antigens showed that the four clones we isolated were positive for CD29, CD90, and CD106 but failed to express the hematopoietic markers CD34, human leukocyte antigen–DR, and CD45 (Fig. 2A, Supporting Information Fig. S3a). When MSCs were subjected to the preinduction medium followed by MNM as described previously [13, 35, 36], they rapidly underwent dramatic morphological changes. Within a few hours, large number of the cells rounded up and showed thin radial processes reminiscent of neurites (Supporting Information Fig. S2ab', c'). After 24 hours of neural induction, most cells presented with neuron-like morphology, including a small-cell body and neurite-like extensions (Fig. 1AB′, Supporting Information Fig. S2ad'). After 48–72 hours of neural induction, neurite-like extensions appeared elongated and fully developed (Supporting Information Fig. S2ae′, f′). Importantly, our RT-PCR analysis revealed that the expression of neural progenitor markers such as Nestin, NeuroD1, Sox-2, and Aquaporin 4 increased concomitantly with the transition of the MSCs into neuronal phenotypes, which peaked at 48–72 hours after induction

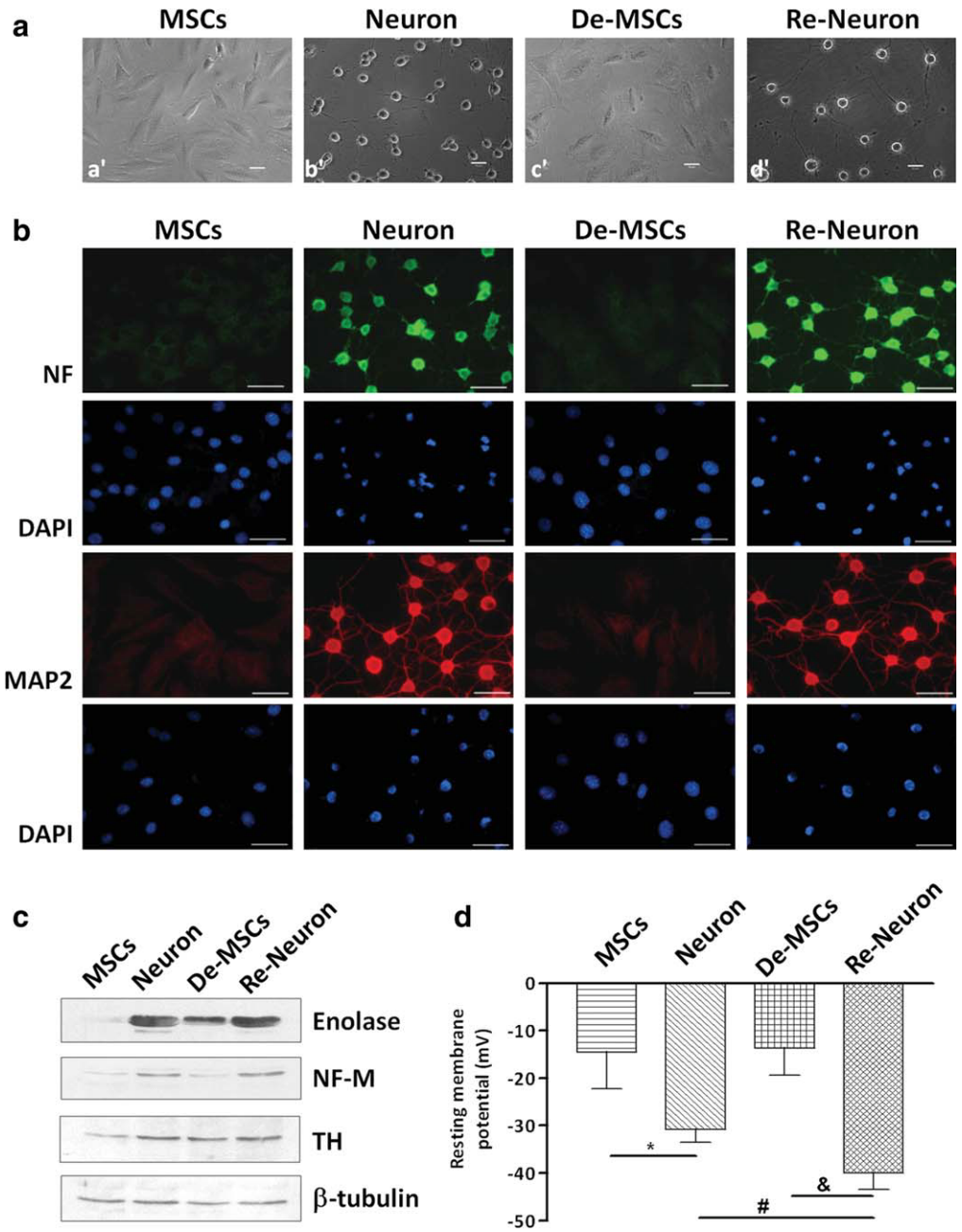

Figure 1. Neuronal differentiation, dedifferentiation, and redifferentiation of monoclonal rat bone marrow MSCs. Monoclonal MSCs (clone 3) were plated at 10×10^2 per centimeter square in six-well plates, and neuronal differentiation, dedifferentiation, and redifferentiation were performed as described in Materials and Methods section. In brief, undifferentiated MSCs were induced in modified neuronal medium (MNM) for 24 hours, washed with PBS, and then reincubated in MSC full media for 24 hours; reinduction was achieved by MNM for another 24 hours. Under these conditions, cells were fixed for immunofluorescence staining or cell lysates were collected for Western blot analysis. **(A):** Phase contrast photographs of neuronal differentiation, dedifferentiation, and redifferentiation of MSCs. Scale bar = 30 μm. (A′): Undifferentiated MSCs; (B′): MSCs rapidly transformed from fibroblastic to neuronal morphology with highly retractile cell bodies and long process-like extensions in MNM; (C′): 24 hours after MNM withdrawal, MSC-derived neuronal morphology was reverted to stromal morphology in 10% FBS; (D′): De-MSCs-derived cells exhibiting neuronal morphology after 24 hours of neuronal reinduction. **(B):** Immunostaining of the general neuronal markers, NF-M and MAP-2, during neuronal differentiation, dedifferentiation, and redifferentiation process with corresponding DAPI staining (scale bar = 50 μm). **(C):** Expression of neuronal markers NSE, NF-M, and TH was examined by Western blot analysis. The variability of protein expression correlated with neuronal differentiation, dedifferentiation, and redifferentiation process. Comparable levels of β-tubulin were detected in each lane, indicating equal loading of samples. **(D):** Resting membrane potential was determined by whole cell patch clamp analysis. Values are presented as mean ± SD (*, $p < .05$, MSCs vs. neuron; &, $p < .05$, De-MSCs vs. re-neuron; #, $p < .05$, neuron vs. re-neuron, Student's t test). Abbreviations: DAPI, 4′,6-diamidino-2-phenylindole; De-MSCs, dedifferentiated MSCs; MSCs, mesenchymal stem cells; MAP, microtubule-associated protein 2; NF-M, neurofilament-M; NSE, neuron-specific enolase; PBS, phosphate-buffered saline; TH, tyrosine hydroxylase.

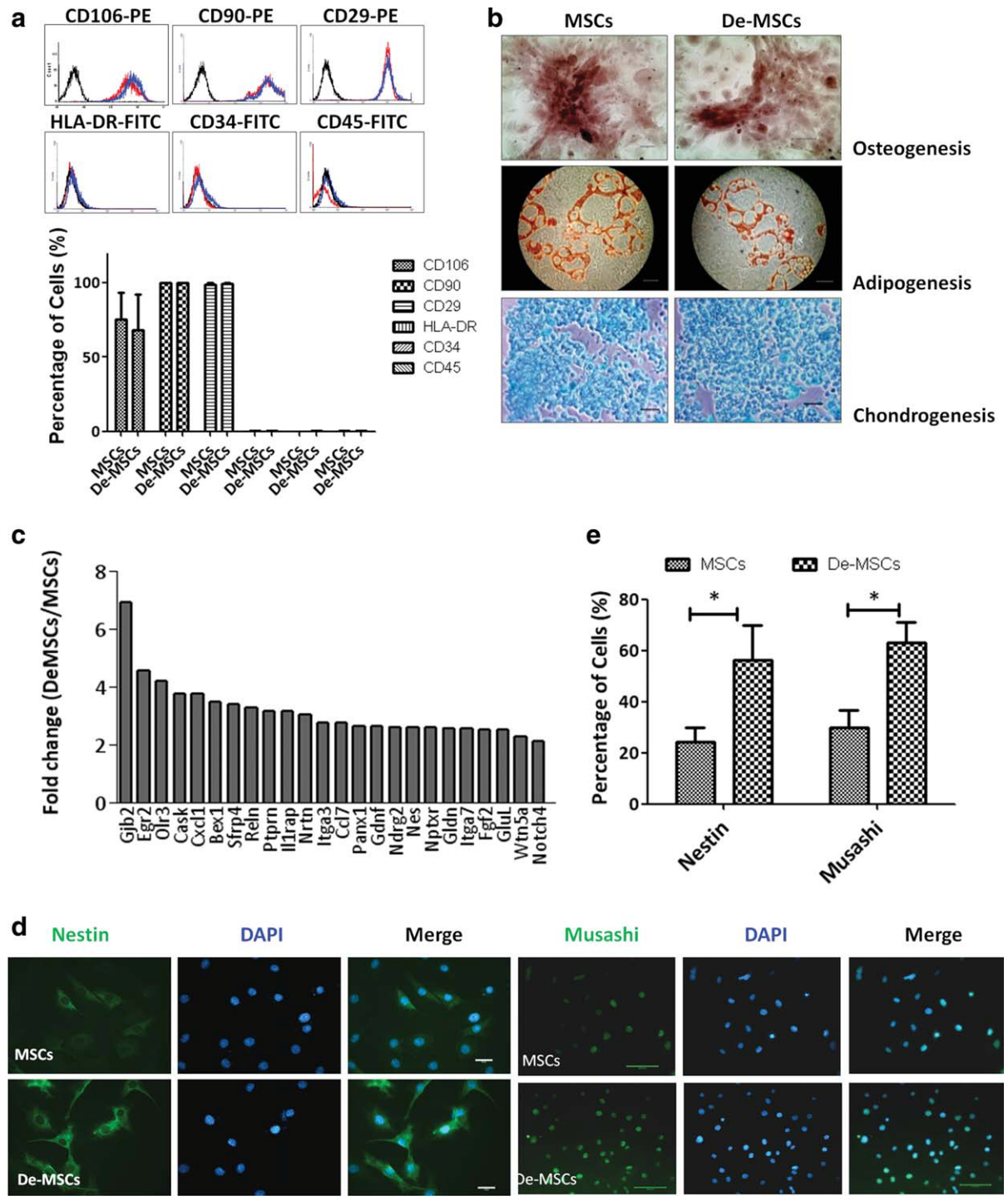

Figure 2. Phenotypic and molecular characterization of De-MSCs. **(A):** Flow cytometry analysis showed that De-MSCs (clone 3) at passage 2 (day 5 after dedifferentiation) retained stem cell surface markers similar to undifferentiated MSCs. Values presented in the lower panel are mean ± SD of three independent experiments. **(B):** Osteogeic, adipogenic, and chondrogenic cells were selectively induced from MSCs and De-MSCs. De-MSCs displayed the same mesenchymal differentiation potential as undifferentiated MSCs (scale bar = 50 μm). **(C):** Comparison of top increased genes involved in neurogenesis between De-MSC (24 hours after dedifferentiation) and MSC populations as assessed by agilent rat whole genome microarray. **(D):** Immunocytochemical analysis of neural progenitor markers, nestin and musashi (scale bar = 30 μm), in MSCs and De-MSCs (24 hours after dedifferentiation). **(E):** The histogram demonstrated the quantification of nestin- and musashi-positive cells in MSC or De-MSC populations. Results were acquired from 10 fields at ×20 magnification. *, $p < .05$. Abbreviations: DAPI, 4′,6-diamidino-2-phenylindole; De-MSCs, dedifferentiated MSCs; FITC, fluorescein isothiocyanate; HLA-DR, human leukocyte antigen–DR; MSCs, mesenchymal stem cells; PE, phycoerythrin.

(Supporting Information Fig. S2b-f). Furthermore, in keeping with the morphological changes, our immunofluorescence analysis showed that the expression of neural cytoskeleton markers neurofilament-M (NF-M) and microtubule-associated protein 2 (MAP2) were barely detectable in uncommitted MSCs, whereas significantly increased after 24-hour neuronal induction (Fig. 1B). However, withdrawal of MNM rapidly reverted MSC-derived neuron-like cells to characteristic mesenchymal morphology and suppressed NF-M and MAP2 expression within 24 hours (Fig. 1AC′, 1B). Intriguingly, these De-MSCs from differentiated neuronal cultures could be reinduced into neuronal phenotype on re-exposure in MNM without preinduction with ATRA and bFGF (Fig. 1AD′). Moreover, virtually 100% of the redifferentiated cells were NF-M- and MAP2-positive (Fig. 1B). Besides, different clones of MSCs were examined for their neuronal differentiation and dedifferentiation capacity. As shown in Supporting Information Figure S3b–d, while different clonally derived MSCs possess variable neuronal differentiation potential, all of them exhibit enhanced cell survival and differentiation potential after dedifferentiation process, indicating that the advantage observed in the De-MSCs represents a general property among different clones.

Neuronal differentiation, dedifferentiation, and redifferentiation of monoclonal MSCs were confirmed by the concomitant upregulation and reversion of multiple neurogenesis marker genes as determined by PCR array (Supporting Information Fig. S4). Transcripts most highly increased during neuronal differentiation and reversed on stimuli withdrawal included genes involved in synaptic functions (*Ache*, *Apoe*, *Grin1*, *Nptx1*, *Pou4f1*, and *S100b*), growth factors and cytokines imperial for neural development (*Bdnf*, *Bmp4*, *Bmp8a*, *Egf*, *Gpi*, *Cxc1*, and *Ptn*), and cell signaling genes involved in neurogenesis and differentiation (*Adora1*, *Adora2*, *bail*, *Cdk5r1*, *Cdk5rap1*, *gnao1*, and *Hey1*). In addition, the neuronal transition and dedifferentiation processes were further verified by our Western blot analysis. As shown in Figure 1C, the expression levels of neuron-specific enolase, NF-M, and rate-limiting enzyme in dopamine synthesis, tyrosine hydroxylase, were markedly increased in differentiated cultures compared with undifferentiated MSCs. Dedifferentiation from the neuronal to the stem cell phenotype was associated with a marked reduction in the expression of neuronal proteins. However, the expression of these neuronal markers in De-MSCs was higher than that in undifferentiated MSCs, suggesting that De-MSCs retained some neuronal traits, and therefore presumably, with higher potential for redifferentiation into neurons. Indeed, De-MSCs could undergo redifferentiation with full expression of the neuronal markers (Fig. 1C).

As excitability is the fundamental property of neurons, which is determined by the resting membrane potential (RMP), we measured the RMP in different groups of MSCs by using whole cell patch clamp as a functional index. As shown in Figure 1D, similar RMP was observed for MSCs and De-MSCs, -14.6 ± 17.055 mV (mean $\pm$ SD, $n = 5$) and -13.667 ± 9.866 mV ($n = 3$), respectively. However, cells derived from MSCs were significantly hyperpolarized after neuronal induction with a RMP of -30.784 ± 11.746 mV ($n = 19$). Interestingly, re-neurons derived from De-MSCs were significantly more hyperpolarized (-39.986 ± 12.840 mV, $n = 14$) than the neuronal progenitors derived from MSCs, indicating that De-MSCs have higher potential to develop into mature functional neurons than MSCs. Taken together, these results validate our in vitro neuronal differentiation and dedifferentiation platform with appropriate culture condition.

De-MSCs Are Distinct from MSCs

Are De-MSCs identical to or different from MSCs? We attempted to address this question first by comparing the cell-surface antigen profiles of De-MSCs at passage 1–3 to those of undifferentiated counterparts. Fluorescence-activated cell sorting (FACS) profiling showed that De-MSCs retained their immunophenotype similar to that of undifferentiated MSCs (Fig. 2A). We then further determined whether De-MSCs are able to maintain their mesodermal differentiation potential after an in vitro differentiation and dedifferentiation procedure. As shown in Figure 2B, both MSCs and De-MSCs could be induced in vitro for 21 days to acquire the typical characteristics of mature osteoblasts, adipocytes, and chondrocytes, indicating that De-MSCs retain mesodermal potential after in vitro neuronal differentiation and dedifferentiation.

Global gene expression profiling has been widely used to identify the transcriptional signatures of specific stem cells. If the dedifferentiation process has reverted the differentiated MSCs to their undifferentiated state, the De-MSCs should possess similar genetic signature as undifferentiated MSCs, or otherwise different. The gene expression profiles of undifferentiated and De-MSCs were compared using Agilent rat whole genome microarray kit, which contains 41,012 oligo probes (Agilent Technologies). The results showed that, in general, 650 (1.5%) genes were upregulated and 1,240 (3.0%) genes were downregulated by more than twofold in De-MSCs compared to undifferentiated MSCs. Transcripts most highly enriched in De-MSCs included imperative genes and growth factors for neural development or neurogenesis (Fig. 2C, *Gjb2*, 6.52-fold; *Egr2*, 4.28-fold; *Olr3*, 3.94-fold; *Nrtn*, 2.87-fold; *Nestin*, 2.46-fold; *Gdnf*, 2.47-fold; *Gldn*, 2.4-fold; *Fgf2*, 2.4-fold; *Glul*, 2.36; *Wnt5a*, 2.16-fold; *Notch* 4, 2.00-fold), indicating that De-MSCs are more committed to a neuronal fate as compared to the undifferentiated MSCs. The expression profiles of some of these genes were confirmed by RT-PCR analysis (Supporting Information Fig. S5a). Conversely, the characteristic genes that are known to be abundantly expressed in MSC, such as *Twist 1*, *Snail2*, *Nidogen 2*, and *Gata6*, are still expressed at the same level in De-MSCs as in undifferentiated MSCs. These results suggest that De-MSCs are similar but not identical to their original counterparts.

Nestin and musashi-1 are widely considered as specific markers of neural stem cells and progenitors [40–42]. Thus, both nestin and musashi-1 expression were investigated as primary markers in undifferentiated MSCs and De-MSCs that would suggest real neuronal potentiality in these cell populations (Fig. 2C, 2D). Immunolabeling analysis demonstrated that $21.7 \pm 5.3\%$ and $29.8 \pm 6.7\%$ of undifferentiated MSCs expressed nestin and musashi, whereas dedifferentiation manipulation markedly increased the number of nestin- and musashi-positive cells to $57.1 \pm 12.2\%$ and $63.2 \pm 7.9\%$ (Fig. 2D). The increase of nestin- and musashi-positive cells in De-MSCs suggests that those cells carried additional neuronal potentiality ready to be activated under appropriate conditions. Taken together, De-MSCs appear to represent a distinct population of stem cells with advanced neuronal potentiality.

Survival Advantage of De-MSCs

Do De-MSCs have significant advantages over undifferentiated MSCs? During the in vitro differentiation and dedifferentiation process, we observed an increase in viable cells in De-MSCs compared with their respective counterparts (Fig. 3A). This could be due to an increase in either cell proliferation and/or survival. Indeed, at 24 hours after dedifferentiation occurred, De-MSCs proliferated vigorously, as illustrated by proliferating cellular nuclear antigen (PCNA) staining (Fig. 3B, Supporting

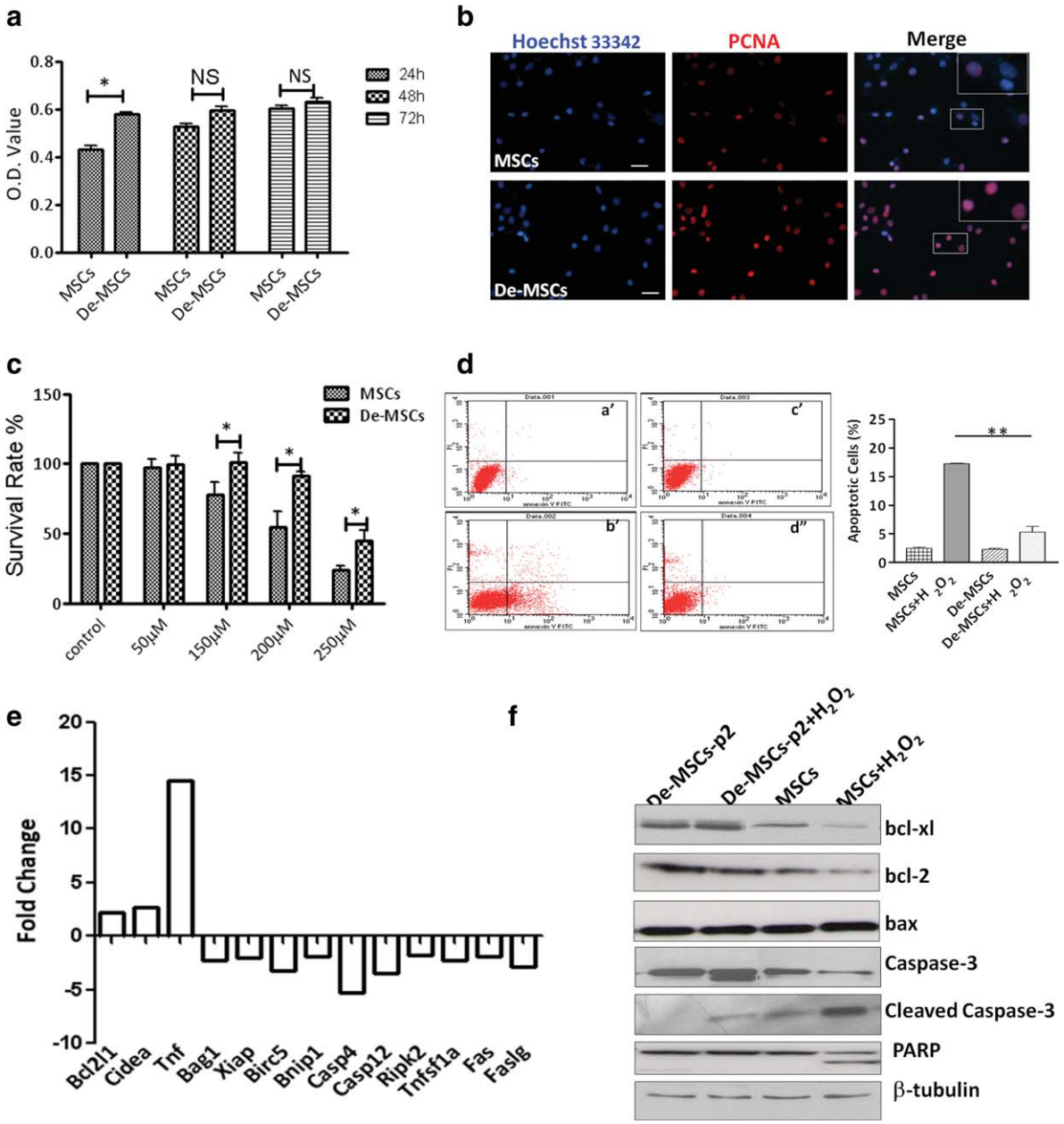

Figure 3. De-MSCs exhibited survival advantage over undifferentiated MSCs. MSCs (clone 3) or De-MSCs were plated at 10×10^2 per centimeter square in six-well plates or 96-well plates, various concentration of H_2O_2 were added to the culture for 24–48 hours as indicated. **(A):** MTS assay showed more viable cells in De-MSC than their respective counterparts after 24 hours of dedifferentiation. However, after 48 and 72 hours of dedifferentiation, there were no significant differences between MSCs and De-MSCs. Values were mean ± SD of three independent experiments (*, $p < .05$, Student's t test). **(B):** A total of 1×10^4 cells were seeded on individual cover slide in six-well plates and stained with PCNA as described in Materials and Methods section. Enhanced PCNA nuclear staining indicates a higher proliferative rate in De-MSCs (24 hours after dedifferentiation) than in MSCs (scale bar = 100 μm). **(C):** MSCs or De-MSCs (24 hours after dedifferentiation) were seeded in 96-well plate 24 hours before challenged with 0–250 μM H_2O_2. De-MSCs had a significantly higher survival rate than MSCs as illustrated by MTS assay. Quantifications shown were mean ± S.D. for six samples from two independent experiments (*, $p < .05$, Student's t-test). **(D):** Fluorescence-activated cell sorting (FACS) analysis of Annexin-V/propidium iodide-stained cells in MSCs and De-MSCs (24 hours after dedifferentiation) challenged with 250 μM H_2O_2 for 24 hours. Primary FACS plots were shown in the upper panel (A′: MSCs; B′: MSCs with H_2O_2; C′: De-MSCs; D′: De-MSCs with H_2O_2), and quantifications from two independent experiments were shown in the lower panel (**, $p < .01$, Student's t test). **(E):** Apoptosis-focused PCR array analysis showed the differentially expressed genes between MSCs and De-MSCs (24 hours after dedifferentiation). Data were analyzed by comparing $2^{-\Delta Ct}$ of the normalized data. Fold changes were calculated relative to the untreated MSCs. The experiments were repeated three times and an arbitrary cut-off of >1.8-fold change and $p < .05$ was used to identify genes that were differentially expressed between samples. **(F):** Cells were treated with 250 μM H_2O_2 for 24 hours. Representative image of Western blot analysis revealed an apparent difference between De-MSCs (passage 2, 5 days after dedifferentiation) and MSCs in terms of bcl-2, bcl-xl, cleaved caspase-3, and cleaved PARP expression under stress. Abbreviations: De-MSCs, dedifferentiated MSCs; MSCs, mesenchymal stem cells; MTS, 3-(4,5-dimethylthiazol-2-yl)-5-(3-carboxymethoxyphenyl)-2-(4-sulfophenyl)-2H-tetrazolium; PCNA, proliferating cellular nuclear antigen; PARP, poly (ADP-ribose) polymerase; PCR, polymerase chain reaction.

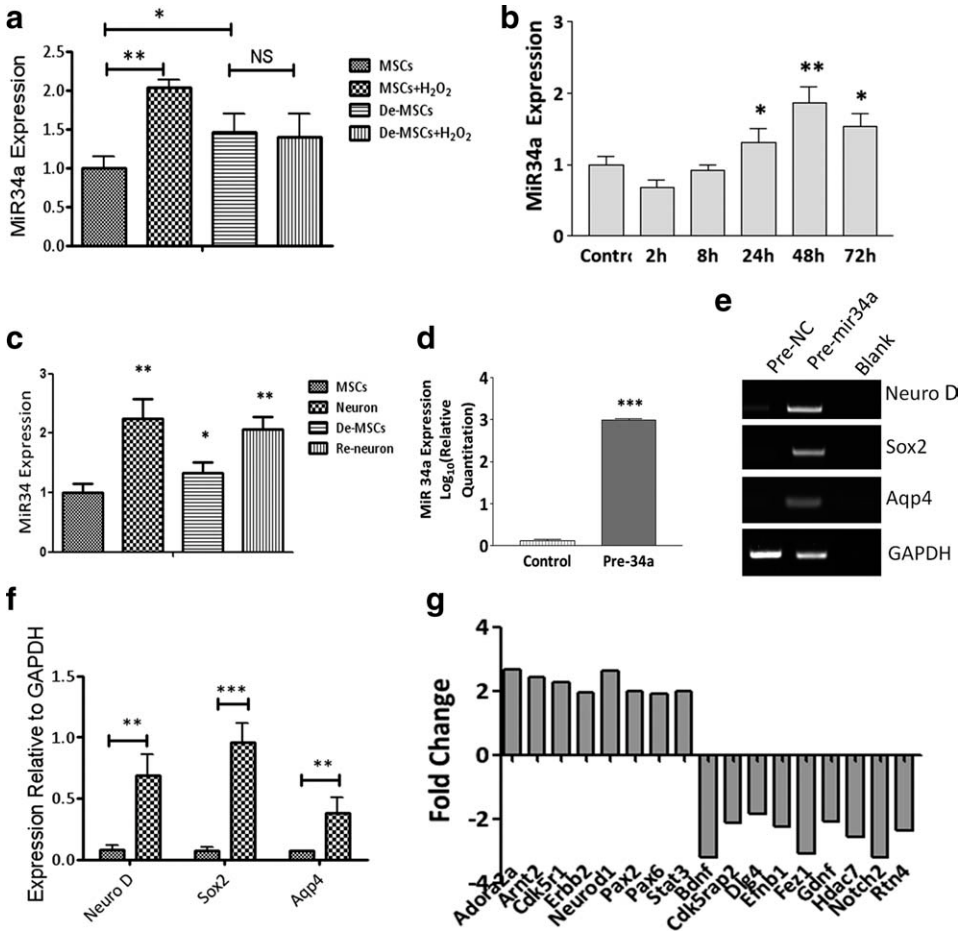

Figure 4. MiR-34a contributed to enhanced neural potentiality in De-MSCs. **(A):** Quantitative PCR (qPCR) analysis of miR34a expression in De-MSCs (24 hours after dedifferentiation) and MSCs with or without H_2O_2 treatment. MSCs or De-MSCs were treated with 250 μM H_2O_2 for 24 hours and RNA was collected and miR-34a expression was determined by qRT-PCR as described in Materials and Methods section (data shown were from triplicate experiments, *, $p < .05$; **, $p < .01$; NS, no significant difference). **(B):** MSCs were induced for neural differentiation in the modified neuronal medium for different time points (24–72 hours), and RNA was collected and miR-34a expression was determined by QRT-PCR. Data shown were from triplicate experiments (*, $p < .05$; **, $p < .01$). **(C):** MSCs underwent neuronal differentiation (24 hours), dedifferentiation (24 hours), and redifferentiation (24 hours); RNA was collected and miR-34a expression was determined by QRT-PCR. Data shown were from triplicate experiments, (*, $p < .05$; **, $p < .01$). **(D):** Pre-miR34a or control-pre-miR was transfected into MSCs as described in Materials and Methods section. After 48 hours of transfection, the cells were lysed and RNA was collected for QRT-PCR (***, $p < .001$). **(E):** Semiquantitative RT-PCR analysis for selected markers of neural stem cells 48 hours after control-pre-miR or pre-miR34a transfected MSCs. Blank indicates cDNA omitted in the reaction. **(F):** Quantificative analysis of (E), data shown were from three independent experiments. **, $p < .01$; ***, $p < .001$. Abbreviations: De-MSCs, dedifferentiated MSCs; MSCs, mesenchymal stem cells; GAPDH, glyceraldehyde 3-phosphate dehydrogenase; PCR, polymerase chain reaction.

Information Fig. S5b, 92.4 ± 4.6% vs. 63.3 ± 8.6%, $p < .05$). However, this proproliferative effect of De-MSCs could not be detected after 48 hours as determined by 3-(4,5-cimethylthiazol-2-yl)-2,5-diphenyl tetrazolium bromide assay (Fig. 3A) or PCNA staining (Supporting Information Fig. S6a,b), indicating the enhanced proliferation might be a result of acute reentry into the cell cycle (Supporting Information Fig. S6c). We also tested possible enhancement in cell survival. While there is nearly no difference detected in spontaneous apoptosis between MSCs and De-MSCs, interestingly, De-MSCs exhibited a survival advantage over undifferentiated MSCs in the condition of oxidative stress. As shown in Figure 3C, there were significantly more viable cells in the De-MSC group than that in the undifferentiated MSC group after hydrogen peroxide (H_2O_2) treatment. Furthermore, this survival advantage in De-MSCs was attributed to their ability to resist H_2O_2-induced apoptosis, as demonstrated by FACS sorting analysis of Annexin-V/propidium iodide staining (Fig. 3D). More importantly, we have found that De-MSCs maintained their antiapoptotis properties after in vitro culture and passaging. As shown in Supporting Information Figure S7, De-MSCs at passage 3 (day 12 after dedifferentiation) maintained enhanced cell survival in response to H_2O_2 as determined by both 3-(4,5-dimethylthiazol-2-yl)-5-(3-carboxymethoxyphenyl)-2-(4-sulfophenyl)-2H-tetrazolium and FACS analysis.

As a first step to identify the genes that contribute to the enhanced survival capacity of De-MSCs, a focused real-time PCR array encompassing 84 genes associated with apoptosis was used. As shown in Figure 3E, 13 of 84 apoptosis-related genes (15.5%) were differentially expressed between MSCs and De-MSCs that reached statistical significance ($p < .05$). Among them, *Bcl-X$_l$*, tumor necrosis factor α (*TNF$_\alpha$*), and *Cidea* were upregulated, whereas the other apoptosis-related genes were downregulated (*Caspases*, inhibitors of apoptosis (*IAPs*), *Fas*, and ligand). Thus, it is likely that complex apoptosis regulation mechanisms may contribute to the difference

between MSCs and De-MSCs. Given the fact that bcl-2 family of proteins is the most prominent gene group involved in cell survival, which is governed at the molecular level by a balance between proapototic and antiapoptotic signals [43], we decided to explore their involvement in the antiapoptotic effects elicited by De-MSCs. Thus, we determined the protein expression of bcl-2, bcl-X_l, and bax on H_2O_2 treatment in both MSCs and De-MSCs. As shown in Figure 3F, while only the transcript of bcl-X_l was enriched in De-MSCs compared to MSCs, protein expression of both bcl-X_l and bcl-2 was upregulated in De-MSCs compared to unmanipulated MSCs. Strikingly, while both bcl-X_l and bcl-2 expression were inhibited by H_2O_2 treatment in MSCs, H_2O_2 challenge did not alter the expression of either bcl-X_l or bcl-2 in De-MSCs, indicating that enhanced expression of bcl-2 family proteins might be responsible for their resistance to H_2O_2 in De-MSCs.

MiR-34a Contributes to Enhanced Cell Survival and Neural Potentiality in De-MSCs

As miR-34a has been reported to be involved in the regulation of apoptosis through direct targeting of bcl-2 [44, 45], we suspected its involvement in underlying the differences in cell survival between De-MSCs and MSCs. Thus, we determined miR-34a expression in both basal and H_2O_2-treated MSCs and De-MSCs. As shown in Figure 4A, miR-34a was markedly increased on H_2O_2 treatment in MSCs whereas there was no change of miR-34a detected in De-MSCs. This result is in line with our finding that bcl-2 is downregulated on H_2O_2 treatment in MSCs but not in De-MSCs. Thus, it appears that the cell survival mechanisms in response to oxidative stress are largely different between MSCs and De-MSCs, which is mostly, if not completely, attributed to miR34a-targeted bcl-2 inhibition.

Intriguingly, we have noticed that De-MSCs exhibited a significantly higher basal level of miR-34a as compared to the original MSCs (Fig. 4A). Although we do not fully understand the mechanisms for this observation, given that De-MSCs exhibit enhanced neuronal differentiation potential and miR-34a has been recently implicated in neuronal differentiation, we speculated that the upregulation of miR-34a could be associated with the advanced neuronal potentiality in De-MSCs. Thus, we determined expression of miR-34a along with neuronal differentiation and dedifferentiation process. As shown in Figure 4B, our qPCR results clearly demonstrated that in keeping with the transition of the stem cells into neuronal phenotypes, miR-34a expression significantly increased in a time-dependent manner. More interestingly, miR-34a expression was altered in concomitant with the neuronal differentiation and dedifferentiation process (Fig. 4C). These results provide us a clue that miR-34a could be involved in the regulation of neurogenesis and contribute to the higher neuronal potentiality observed in De-MSCs. Indeed, ectopic overexpression of miR-34a in MSCs lead to a significant increase of three neural stem cell marker genes, which were also observed to be upregulated in the De-MSCs compared to MSCs. (Fig. 4D, 4E). Moreover, we compared neurogenesis gene expression profiles between control-miR and pre-miR-34a-transfected MSCs using PCR array. Interestingly, our results demonstrated that miR-34a regulated multiple genes involved in the neuronal differentiation (Fig. 4F), further pinpointing the regulatory role of miR-34a in the neural potentiality of MSCs.

De-MSCs Exhibit Enhanced Therapeutic Potential

Do De-MSCs exhibit enhanced therapeutic potential over that of MSCs? As a first step to answer this question, cultures of PHNs were exposed to different concentrations of H_2O_2 for 2 hours followed by coculture with MSCs or De-MSCs for 24 hours. After H_2O_2 exposure, PHN underwent rapid cytoskeleton disaggregation and axonal fragmentation with a significant reduction in viable cells. Coculture with either MSCs or De-MSCs dramatically increased the number of viable cells after different strength of H_2O_2 challenge, with significantly larger number of cells observed in coculture with De-MSCs as compared to that with MSCs (Fig. 5A), indicating enhanced cell survival. Interestingly, we observed that a portion of MSCs or De-MSCs displayed neuronal morphology with contracted multipolar/biopolar cell bodies and process-like extension after 24 hours of coculture (Supporting Information Fig. S9). To identify the cell origin, we used GFP-MSCs or GFP-De-MSCs to coculture with H_2O_2-treated PHN and the results showed that there were more GFP-De-MSCs stained positive with NF-M as compared to GFP-MSCs after coculture with PHN ($90.6 \pm 1.6\%$ vs. $67.1 \pm 5.6\%$, $p < .05$, in 100 μM H_2O_2 group and $90.3 \pm 3.1\%$ vs. $49.5 \pm 6.4\%$, $p < .05$, in 250 μM H_2O_2 group; Fig. 5B-5F), indicating greater neuronal differentiation potential in De-MSCs under stress.

We went further to demonstrate the therapeutic advantage of De-MSCs in vivo in a rat model of neonatal HIBD, which is a common cause of long-term neurological disability in children with no effective treatments available at present. Occlusion of unilateral common carotid artery was produced in 7-day postnatal rats to induce hypoxia, and the effects of transplantation of MSCs and De-MSCs via lateral ventricles were examined. While both transplanted GFP-MSCs and De-MSCs were readily found near the injection sites by their green fluorescence 3 days after transplantation, GFP expression could only be detected in De-MSCs group 7 days after transplantation (Fig. 6A), indicating improved cell survival. On day 3, immunohistochemical analysis on brain sections showed that there was barely obvious colocalization of NF-M (Fig. 6B) or MAP-2 (Supporting Information Fig. S10) with GFP-labeled MSCs or De-MSCs. On day 7, the majority of the survived GFP-De-MSCs were found near the lateral ventricle, but a number of cells were also found outside of the injection site, indicating migration of the cells. Immunostaining revealed that some GFP-positive De-MSCs expressed differentiated neuronal markers NF-M (Fig. 6B) or MAP2 (Supporting Information Fig. S10), indicating neuronal differentiation from the De-MSCs in vivo. Taken together, these results indicated that De-MSCs had survival and neuronal differentiation advantages over undifferentiated MSCs under both in vitro and in vivo conditions.

As MSCs have been implicated in promoting endogenous angiogenesis after injury [46], we also suspected that the better survival of De-MSCs might lie in their greater ability to promote angiogenesis in the ischemic region, without which repair is impossible. We stained ischemic brain tissue with endothelial marker CD31 in both control and stem cell-treated groups 7 days after treatment. Our results demonstrated that the number of CD31-positive vessels increased significantly in the stem cell-transplanted groups compared with the control group. Interestingly, the quantitative analysis showed a significant increase in vessel density in the De-MSC-treated group compared with the MSC group (Fig. 6C). Of note, we observed that some GFP-positive cells in De-MSC group were immunoreactive to CD31, indicating that transplanted De-MSCs might have been transformed into endothelial cells or formed fusion cells with pre-existing endothelial cells. These results suggest that De-MSCs may be more pluripotent as compared to undifferentiated MSCs in promoting angiogenesis, which may contribute to their better survival in the ischemic region.

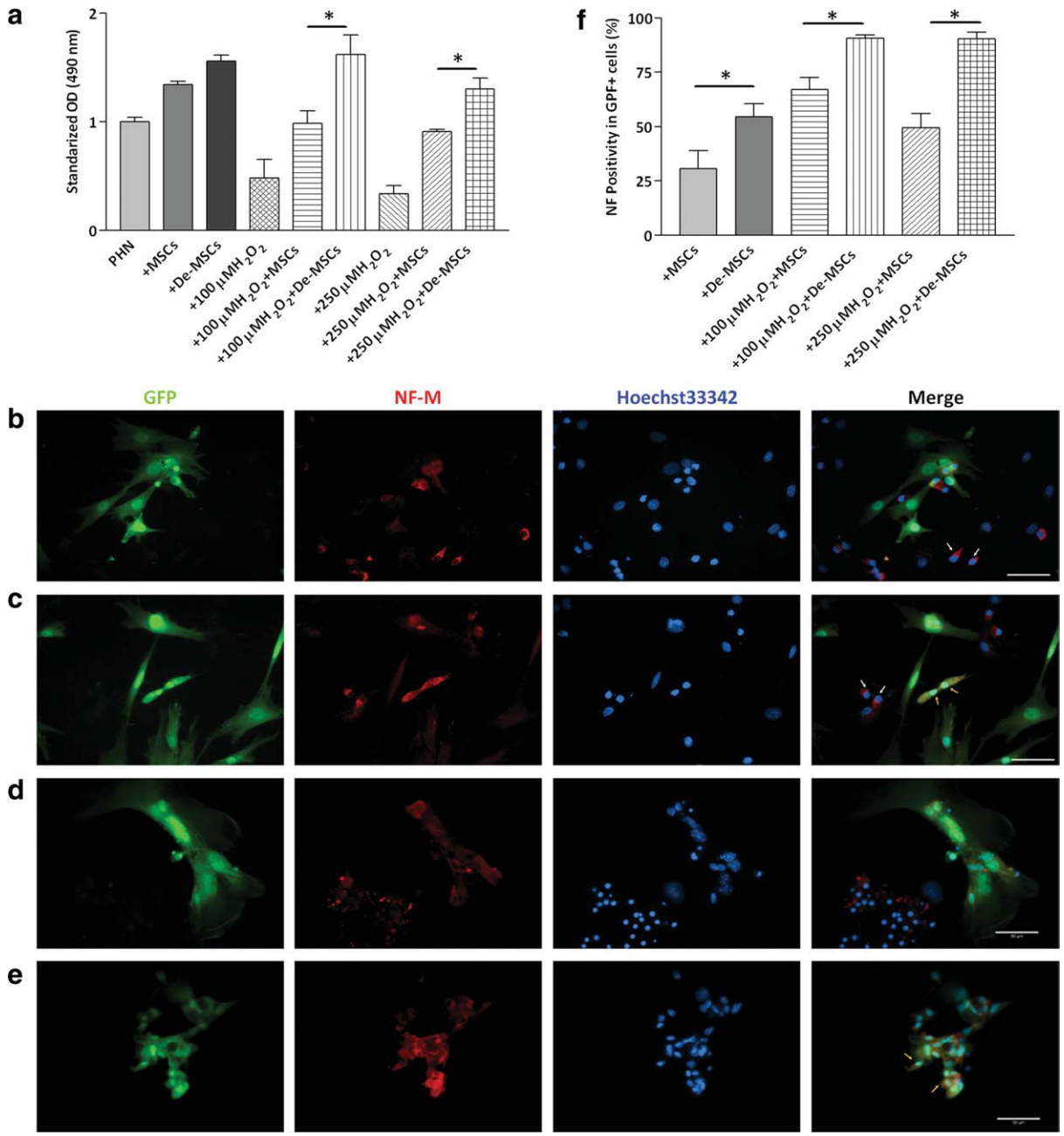

Figure 5. De-MSCs exhibited enhanced survival and neuronal differentiation when cocultured with PHN. Primary cultures of PHN isolated from 1-day-old Sprague-Dawley rat were treated with 100 μM or 250 μM H_2O_2 for 24 hours, washed with PBS, and then cocultured with GFP-expressing MSCs or De-MSCs (24 hours after dedifferentiation) for another 24 hours. **(A):** MTS assay showed more viable cells in H_2O_2-treated PHN cocultured with De-MSCs than that with MSCs. Values were mean ± SD (*, $p < .05$, Student's t test). **(B–E):** Immunostaining of NF-M in H_2O_2-treated PHN cocultured with GFP-MSCs or GFP-De-MSCs for 24 hours (scale bar = 50 μm). (B): PHN cocultured with GFP-MSCs; (C), PHN cocultured with GFP-De-MSCs; (D), 100 μM H_2O_2 treated PHN cocultured with MSCs; (E), 100 μM H_2O_2 treated PHN cocultured with De-MSCs (scale bar = 50 μm). **(F):** Quantification of GFP-MSCs or GFP-De-MSCs expressing NF-M after coculture with PHN for 24 hours. Results were from two independent experiments and analyzed from 20 individual fields (*, $p < .05$, Student's t test). Abbreviations: De-MSCs, dedifferentiated MSCs; GFP, green fluorescent protein; MSCs, mesenchymal stem cells; MTS, 3-(4,5-dimethylthiazol-2-yl)-5-(3-carboxymethoxyphenyl)-2-(4-sulfophenyl)-2H-tetrazolium; NF-M, neurofilament-M; OD, optical density; PBS, phosphate-buffered saline; PHN, primary hippocampal neuron.

We also compared the functional recovery of the HIBD animals after treatment of MSCs and De-MSCs using shuttle box tests, a well-established method for evaluating memory and learning abilities in rodents [39] (Supporting Information Fig. S11). As shown in Figure 6D, animals in all experimental groups exhibited a gradual improvement in cognitive function during the 2-month recovery period. Compared to PBS group ($n = 10$), MSCs ($n = 10$) and De-MSCs ($n = 8$) groups showed more active avoidance response (AAR) in each session and less passive escape response from second session, suggesting that the treatment with MSCs or De-MSCs remarkably improved the cognitive function in HIBD rats.

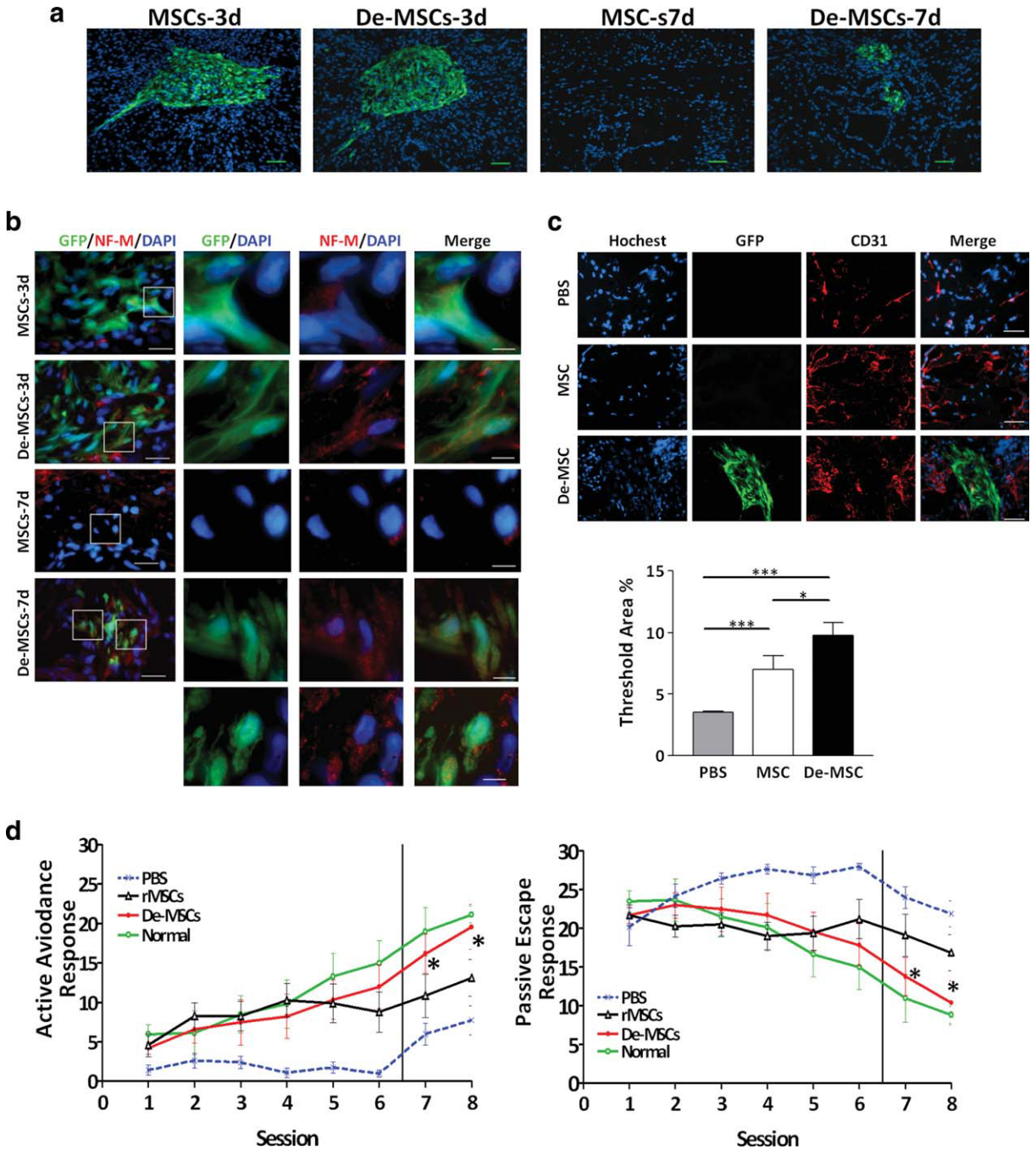

Figure 6. Improved therapeutic effect with transplantation of De-MSCs in HIBD rat model. HIBD rat model was established as described in Materials and Methods section. At 5 days after hypoxia–ischemia, the pups were randomly divided into three groups and infused with 1–2 $\times$ 10^5 MSCs or De-MSCs (24 hours after dedifferentiation) into the right lateral cerebral ventricle. **(A):** Representative photographs showing GFP-expressing MSC or De-MSC on day 3 and day 7 in brain sections after implantation (scale bar = 50 μm). **(B):** Immunohistochemical staining of NF-M on day 3 and day 7 brain sections of HIBD rat transplanted with MSCs or De-MSCs (scale bar = 20 μm). The white box in left panel marks the area enlarged in right panel (scale bar = 5 μm). **(C):** Immunohistochemical staining of CD 31 on day 7 brain sections of HIBD rat transplanted with MSCs or De-MSCs (scale bar = 37.5 μm). Quantification results were analyzed from at least five individual fields and presented as mean $\pm$ SEM. (*, $p < .05$, ***, $p < .01$, one-way ANOVA). **(D):** De-MSCs exhibited enhanced therapeutic effects in shuttle box test. After 5 days of hypoxia–ischemia, the pups were randomly divided into three groups and infused with 1–2 $\times$ 10^5 MSCs or De-MSCs in 5 μL of PBS into the right lateral cerebral ventricle. After 1 month engraftment, the shuttle box tests were performed in MSCs or De-MSCs treated rats. The tests were performed in six continuous sessions for 6 days, and the seventh, eighth sessions were followed 1 and 2 months later, respectively. In the seventh and eighth session performed 1 and 2 months after injury, respectively, the numbers of AAR of injured rats treated with De-MSCs were significantly higher than that with MSCs, showing significant increase in active avoidance and decrease in passive escape in De-MSCs as compared to MSCs-treated groups. Note that the values observed with De-MSCs are not significantly different from that obtained from the normal control, suggesting significant repair by De-MSC treatment (*, $p < .05$, De-MSCs vs. MSCs). Abbreviations: AAR, active avoidance response; DAPI, 4′,6-diamidino-2-phenylindole; De-MSCs, dedifferentiated MSCs; GFP, green fluorescent protein; HIBD, hypoxic-ischemic brain damage; MSCs, mesenchymal stem cells; NF-M, neurofilament-M; PBS, phosphate-buffered saline.

Intriguingly, in the seventh and eighth sessions performed 1 and 2 months after injury, respectively, the numbers of AAR of injured rats treated with De-MSCs were significantly higher than that with MSCs and were not significantly different from those of control rats. These results indicate that De-MSCs are superior to undifferentiated MSCs in repairing brain injury with improved long-term memory retention.

DISCUSSION

Despite being morphologically and phenotypically similar to uncommitted MSCs, De-MSCs, as demonstrated in this study, represent a previously undescribed distinct population of stem cells with several distinguished features and improved therapeutic potential. Notably, apart from the potential for multilineage differentiation into osteoblasts, adipocytes and chondrocytes, De-MSCs exhibit a predisposition to the neuronal lineages as demonstrated by both genetic and functional assays. Global gene expression profiling and PCR data show that dedifferentiated cells express increased level of both neurogenesis-related genes and growth factors (Fig. 2C, Supporting Information Fig. S5a). Conversely, it should be noted that various neural stem cell markers such as Nestin, Musashi, NeuroD1, Sox-2, and Aqp4 increase dramatically in a time-dependent manner with the transition of the MSCs into neuronal phenotypes (Supporting Information Fig. S2, Fig. 2D). These data indicate that MSC-derived cells have committed to neural lineage and represent an immature neural phenotype, most likely neural stem/progenitor cells. This notion is further supported by our observation that the methylation status of H3K4me3 and H3K27me3 in De-MSCs is similar to differentiated neurons rather than uncommitted MSCs (Supporting Information Fig. S5b). Although the question of how the epigenetic state of a cell influences fate determination has been previously addressed on ESCs, recent investigations focused on the role of epigenetic regulation in lineage-specific differentiation of MSCs have shown that unique patterns of DNA methylation and histone modifications play an important role in the induction of MSC differentiation toward specific lineages [47, 48]. Particularly, it has been demonstrated that the modifiers of histone methylation can efficiently promote the generation of neural cells from MSCs [49, 50]. Therefore, although the precise association of histone methylation with differentiation potential in MSCs and De-MSCs will need to be determined more extensively in future studies, the differences in histone methylation observed between MSC and De-MSC suggest that epigenetic mechanisms are probably involved in determining the differentiation potential of these two populations.

Apart from that, De-MSCs appear to offer therapeutic advantages in that they are more resistant to hostile environment as illustrated by injured PHN coculture and HIBD animal model (Figs. 5, 6). The presently demonstrated higher survival rate of De-MSCs could be explained by their increased expression of bcl-2 family genes including bcl-x_l and bcl-2. Both bcl-x_l and bcl-2 have been well-established to play antiapoptotic action in various cellular context [51]. Interestingly, recent studies have shown that transplantation with Bcl-2 family gene modified MSCs resulted in enhanced cell survival and functional improvement in rat ischemic models [52] as all stem cells engrafted into diseased tissue will commonly be exposed to a hostile pathological environment, such as hypoxia, low serum, oxidative stress. De-MSCs with higher endogenous bcl-2 and bcl-x_l expression should offer significant advantages over unmanipulated MSCs. Of note, while we did not observe any significant difference in bcl-2 family proteins between MSCs and De-MSCs on serum deprivation (Supporting Information Fig. S8), our Western blot analysis demonstrated that on H_2O_2 treatment, the expression level of both bcl-x_l and bcl-2 was inhibited in MSCs, but not in De-MSCs (Fig. 3F). These results indicate that serum deprivation and H_2O_2 trigger distinctive apoptotic pathways in MSCs, and bcl-2 family genes are differentially regulated on oxidative stress in MSCs and De-MSCs. On top of that, we have observed that various TNF superfamily members are also differentially expressed between MSCs and De-MSCs. Among them, TNF_α is dramatically increased whereas TNFsf1a (TNF_α receptor 1), Fas and FasL are decreased in De-MSCs compared to MSCs (Fig. 3E). The function of TNF_α is ambiguous in various cell types because TNF_α is mediated by two receptors with different activation paths [53]. The activation of TNF receptor 1 has been reported to decrease MSC growth factor production [54], generate reactive oxygen species, and induce apoptosis [55] whereas TNF receptor 2 has been demonstrated to enhance MSC growth through the activation of NF-κB [56]. Conversely, it has been shown that fetal and adult MSCs are killed by different pathways; in particular, fetal MSCs are preferably killed via TNF_α while the adult MSCs are more sensitive to FasL pathway [57]. More intriguingly, a recent study has revealed that TNF_α by its own can specify human MSCs to a neural fate [58]. Based on these findings, while the final biological significance of these TNF family members in the complex apoptosis mechanism of MSCs is still elusive, we speculate that the enhanced survival in De-MSCs might be related to the downregulation of TNF receptor 1 and Fas pathway, which requires further investigation in future.

In addition to the demonstrated enhanced cell survival and neuronal differentiation, De-MSCs, compared to unmanipulated MSCs, may also propel local microenvironmental signals to better sustain active endeavors for damaged neuron substitution, normally failing in nonsupportive pathological surroundings. In fact, stimulation of endogenous repair mechanisms in ischemic brain has been suggested to be a novel and promising therapeutic application of MSCs despite their limited survival and differentiation potential in vivo [59], which may be accounted for the presently observed therapeutic effect of MSCs in HIBD model. Interestingly, we also observed that De-MSC-treated animals had greater angiogenesis near the border of the ischemic lesions (Fig. 6C), which may contribute to the observed better survival of De-MSCs in HIBD model. Consistent with this notion, the global gene expression profiles of De-MSCs or MSCs-treated injured cerebral hemisphere 1 week after transplantation showed that there were 41 genes upregulated and 331 genes downregulated at least twofold in De-MSCs group compared to MSCs group. Assessment of the gene ontology designations of these genes found several pathways to be significantly over-represented, in particular, pathways involved in stress response, immune response as well as cytokine activity (Supporting Information Fig. S12). It is very likely that De-MSCs also exert endogenous repair mechanisms, including angiogenesis, with advantages distinct from that of undifferentiated MSCs.

The recently demonstrated dedifferentiation capacity from terminally differentiated mammalian somatic cells via genetic manipulations to induced pluripotent stem cells (iPSCs) has great impact on cell-based therapy [60–62]. The cells are forced to express specific transcription factors, such as *Oct4*, *Sox-2*, *c-Myc*, and *Klf4*, and subsequently reprogrammed to exhibit features reminiscent of embryonic stem cells, termed iPS. Here we have demonstrated that withdrawal of induction media and reincubation in serum is sufficient to reprogram the neuronal lineage-committed cells back to multipotent

cells. Interestingly, none of the four genes reported to be important to induce iPS has found to be altered in their expression in De-MSCs, indicating that the molecular mechanisms underlying the dedifferentiation or reprogramming may be different from those reported to induce embryonic stem cell-like iPS. In an attempt to identify the potential molecular mechanisms contributing to the dedifferentiation phenotype, we found that De-MSCs express higher level of miR-34a. Moreover, our results have shown that H_2O_2 dramatically upregulates miR-34a expression in MSCs but not in De-MSCs (Fig. 4C). As miR-34a, which is a direct target of *p53*, has been well-characterized as an apoptosis executor through direct targeting of apoptosis-related genes including bcl-2, it is very likely that the distinctive regulation of miR-34a accounts for the differential apoptosis mechanism observed between MSCs and De-MSCs on oxidative stress. Conversely, a role for miR-34a in cell differentiation has been recently reported [63–65]. Intriguingly, Aranha et al. has demonstrated that overexpression of miR-34a increases the proportion of postmitotic neurons in distinct models of neural differentiation including mouse embryonic stem cells and neural stem cells. In this study, as we observed that the alteration of miR-34a expression coincided with the neuronal differentiation and dedifferention process (Fig. 4A, 4B), we investigated the effect of miR-34a upregulation on the neural potential of MSCs. Interestingly, we have demonstrated that ectopic expression of pre-miR-34a in MSCs significantly increases the expression of multiple neural stem cell as well as neurogenesis-related markers, mimicking the molecular signatures that observed in De-MSCs (Fig. 4D-4G). Taken together, these results have suggested a pivotal role of miR-34a in regulating cell survival and neuronal differentiation in MSCs, alteration of which may contribute to the reprogramming and differences observed between De-MSCs and MSCs. Together with the high levels of H3K4me3 and H3K27me3 found in De-MSCs, both of which are related to stem cell survival and fate decision [66], we propose that epigenetic regulation may be one of the key mechanisms underlying the reprogramming by dedifferentiation in MSCs.

Conclusion

In conclusion, this study has characterized a previously undescribed dedifferentiation-reprogrammed stem cell population that exhibits enhanced cell survival and differentiation with improved therapeutic potential in vitro and in vivo. With easy culture manipulation and low tendency of tumor formation, as compared to the more complicated genetic manipulation and higher risk of iPS forming teratomas on transformation [67], De-MSCs may offer at least two advantages over iPS in cell-based therapy. The presently demonstrated advantages and improved therapeutic potential of De-MSC warrant further investigation into this distinct stem cell population and the detailed mechanism underlying the dedifferentiation-induced reprogramming process.

Acknowledgments

This work was supported in part by the Focused Investment Scheme and Li Ka Shing Institute of Health Sciences of the Chinese University of Hong Kong, Morningside Foundation, National Natural Science Foundation of China (Nos. 30830106, 30872670, and 81100475), National Basic Research Program of China (2012CB944900), Fundamental Research Funds for the Central Universities (Jinan University). Xiaohua Jiang is supported by Direct Grants (2009.1.071, 2010.1.016) of the Chinese University of Hong Kong, GRF2010/2011 (CUHK466710) of Hong Kong University Grants Committee, and NSFC grant 31140034.

Disclosure of Potential Conflict of Interest

The authors indicate no potential conflicts of interest.

References

1 Prockop DJ. Marrow stromal cells as stem cells for nonhematopoietic tissues. Science 1997;276:71–74.
2 Pittenger MF, Mackay AM, Beck SC et al. Multilineage potential of adult human mesenchymal stem cells. Science 1999;284:143–147.
3 Brazelton TR, Rossi FM, Keshet GI et al. From marrow to brain: Expression of neuronal phenotypes in adult mice. Science 2000;290: 1775–1779.
4 Mezey E, Chandross KJ, Harta G et al. Turning blood into brain: Cells bearing neuronal antigens generated in vivo from bone marrow. Science 2000;290:1779–1782.
5 Joshi CV, Enver T. Plasticity revisited. Curr Opin Cell Biol 2002;14: 749–755.
6 Jiang Y, Jahagirdar BN, Reinhardt RL et al. Pluripotency of mesenchymal stem cells derived from adult marrow. Nature 2002;418: 41–49.
7 Orlic D, Kajstura J, Chimenti S et al. Bone marrow cells regenerate infarcted myocardium. Nature 2001;410:701–705.
8 Hattan N, Kawaguchi H, Ando K et al. Purified cardiomyocytes from bone marrow mesenchymal stem cells produce stable intracardiac grafts in mice. Cardiovasc Res 2005;65:334–344.
9 Shim WS, Jiang S, Wong P et al. Ex vivo differentiation of human adult bone marrow stem cells into cardiomyocyte-like cells. Biochem Biophys Res Commun 2004;324:481–488.
10 Petersen BE, Bowen WC, Patrene KD et al. Bone marrow as a potential source of hepatic oval cells. Science 1999;284:1168–1170.
11 Lee KD, Kuo TK, Whang-Peng J et al. In vitro hepatic differentiation of human mesenchymal stem cells. Hepatology 2004;40: 1275–1284.
12 Lin Y, Weisdorf DJ, Solovey A et al. Origins of circulating endothelial cells and endothelial outgrowth from blood. J Clin Invest 2000; 105:71–77.
13 Woodbury D, Schwarz EJ, Prockop DJ et al. Adult rat and human bone marrow stromal cells differentiate into neurons. J Neurosci Res 2000;61:364–370.
14 Qian L, Saltzman WM. Improving the expansion and neuronal differentiation of mesenchymal stem cells through culture surface modification. Biomaterials 2004;25:1331–1337.
15 Levy YS, Stroomza M, Melamed E et al. Embryonic and adult stem cells as a source for cell therapy in Parkinson's disease. J Mol Neurosci 2004;24:353–386.
16 Rismanchi N, Floyd CL, Berman RF et al. Cell death and long-term maintenance of neuron-like state after differentiation of rat bone marrow stromal cells: A comparison of protocols. Brain Res 2003;991: 46–55.
17 Park HJ, Lee PH, Bang OY et al. Mesenchymal stem cells therapy exerts neuroprotection in a progressive animal model of Parkinson's disease. J Neurochem 2008;107:141–151.
18 Li Y, Chopp M, Chen J et al. Intrastriatal transplantation of bone marrow nonhematopoietic cells improves functional recovery after stroke in adult mice. J Cereb Blood Flow Metab 2000;20: 1311–1319.
19 Li Y, Chen J, Wang L et al. Treatment of stroke in rat with intracarotid administration of marrow stromal cells. Neurology 2001;56: 1666–1672.
20 Chen J, Li Y, Wang L et al. Therapeutic benefit of intravenous administration of bone marrow stromal cells after cerebral ischemia in rats. Stroke 2001;32:1005–1011.
21 Hofstetter CP, Schwarz EJ, Hess D et al. Marrow stromal cells form guiding strands in the injured spinal cord and promote recovery. Proc Natl Acad Sci USA 2002;99:2199–2204.

22 Jin HK, Carter JE, Huntley GW et al. Intracerebral transplantation of mesenchymal stem cells into acid sphingomyelinase-deficient mice delays the onset of neurological abnormalities and extends their life span. J Clin Invest 2002;109:1183–1191.
23 Li Y, Chen J, Chen XG et al. Human marrow stromal cell therapy for stroke in rat: Neurotrophins and functional recovery. Neurology 2002; 59:514–523.
24 Swanger SA, Neuhuber B, Himes BT et al. Analysis of allogeneic and syngeneic bone marrow stromal cell graft survival in the spinal cord. Cell Transplant 2005;14:775–786.
25 Odelberg SJ, Kollhoff A, Keating MT. Dedifferentiation of mammalian myotubes induced by msx1. Cell 2000;103:1099–1109.
26 Brockes JP. Amphibian limb regeneration: Rebuilding a complex structure. Science 1997;276:81–87.
27 Brockes JP, Kumar A. Plasticity and reprogramming of differentiated cells in amphibian regeneration. Nat Rev Mol Cell Biol 2002;3: 566–574.
28 Walsh K, Perlman H. Cell cycle exit upon myogenic differentiation. Curr Opin Genet Dev 1997;7:597–602.
29 Hu G, Lee H, Price SM et al. Msx homeobox genes inhibit differentiation through upregulation of cyclin D1. Development 2001;128: 2373–2384.
30 Tsai RY, Lee SH, Chan HL. The distribution of follicular units in the Chinese scalp: Implications for reconstruction of natural-appearing hairlines in Orientals. Dermatol Surg 2002;28:500–503.
31 Clarke DL, Johansson CB, Wilbertz J et al. Generalized potential of adult neural stem cells. Science 2000;288:1660–1663.
32 Liang L, Bickenbach JR. Somatic epidermal stem cells can produce multiple cell lineages during development. Stem Cells 2002;20:21–31.
33 McGann CJ, Odelberg SJ, Keating MT. Mammalian myotube dedifferentiation induced by newt regeneration extract. Proc Natl Acad Sci USA 2001;98:13699–13704.
34 Zhang Y, Li TS, Lee ST et al. Dedifferentiation and proliferation of mammalian cardiomyocytes. PLoS ONE 2010;5:e12559.
35 Woodbury D, Reynolds K, Black IB. Adult bone marrow stromal stem cells express germline, ectodermal, endodermal, and mesodermal genes prior to neurogenesis. J Neurosci Res 2002;69:908–917.
36 Li TY, Shu C, Wong CH et al. Plasticity of rat bone marrow-derived 5-hydroxytryptamine-sensitive neurons: Dedifferentiation and redifferentiation. Cell Biol Int 2004;28:801–807.
37 Sheng H, Zhang Y, Sun J et al. Corticotropin-releasing hormone (CRH) depresses *n*-methyl-D-aspartate receptor-mediated current in cultured rat hippocampal neurons via CRH receptor type 1. Endocrinology 2008;149:1389–1398.
38 Rice JE, 3rd, Vannucci RC, Brierley JB. The influence of immaturity on hypoxic-ischemic brain damage in the rat. Ann Neurol 1981;9: 131–141.
39 Ahlenius S, Engel J, Lundborg P. Antagonism by d-amphetamine of learning deficits in rats induced by exposure to antipsychotic drugs during early postnatal life. Naunyn Schmiedebergs Arch Pharmacol 1975;288:185–193.
40 Nunes MC, Roy NS, Keyoung HM et al. Identification and isolation of multipotential neural progenitor cells from the subcortical white matter of the adult human brain. Nat Med 2003;9:439–447.
41 Toma JG, Akhavan M, Fernandes KJ et al. Isolation of multipotent adult stem cells from the dermis of mammalian skin. Nat Cell Biol 2001;3:778–784.
42 Kaneko Y, Shimada K, Saitou K et al. The mechanism responsible for the drowsiness caused by first generation H1 antagonists on the EEG pattern. Methods Find Exp Clin Pharmacol 2000;22:163–168.
43 Dietrich JB. Apoptosis and anti-apoptosis genes in the Bcl-2 family. Arch Physiol Biochem 1997;105:125–135.
44 Chang TC, Wentzel EA, Kent OA et al. Transactivation of miR-34a by p53 broadly influences gene expression and promotes apoptosis. Mol Cell 2007;26:745–752.
45 Raver-Shapira N, Marciano E, Meiri E et al. Transcriptional activation of miR-34a contributes to p53-mediated apoptosis. Mol Cell 2007;26: 731–743.
46 Toyama K, Honmou O, Harada K et al. Therapeutic benefits of angiogenetic gene-modified human mesenchymal stem cells after cerebral ischemia. Exp Neurol 2009;216:47–55.
47 Hassan MQ, Tare R, Lee SH et al. HOXA10 controls osteoblastogenesis by directly activating bone regulatory and phenotypic genes. Mol Cell Biol 2007;27:3337–3352.
48 Fan Z, Yamaza T, Lee JS et al. BCOR regulates mesenchymal stem cell function by epigenetic mechanisms. Nat Cell Biol 2009;11:1002–1009.
49 Alexanian AR. Epigenetic modifiers promote efficient generation of neural-like cells from bone marrow-derived mesenchymal cells grown in neural environment. J Cell Biochem 2007;100:362–371.
50 Alexanian AR. An efficient method for generation of neural-like cells from adult human bone marrow-derived mesenchymal stem cells. Regen Med 2010;5:891–900.
51 Fleischer A, Ghadiri A, Dessauge F et al. Modulating apoptosis as a target for effective therapy. Mol Immunol 2006;43:1065–1079.
52 Li W, Ma N, Ong LL et al. Bcl-2 engineered MSCs inhibited apoptosis and improved heart function. Stem Cells 2007;25:2118–2127.
53 Wallach D. Neutrophilic disease. Rev Prat 1999;49:356–358.
54 Markel TA, Crisostomo PR, Wang M et al. Right ventricular TNF resistance during endotoxemia: The differential effects on ventricular function. Am J Physiol Regul Integr Comp Physiol 2007;293: R1893–R1897.
55 Schutze S, Tchikov V, Schneider-Brachert W. Regulation of TNFR1 and CD95 signalling by receptor compartmentalization. Nat Rev Mol Cell Biol 2008;9:655–662.
56 Miettinen JA, Pietila M, Salonen RJ et al. Tumor necrosis factor alpha promotes the expression of immunosuppressive proteins and enhances the cell growth in a human bone marrow-derived stem cell culture. Exp Cell Res 2011;317:791–801.
57 Gotherstrom C, Lundqvist A, Duprez IR et al. Fetal and adult multipotent mesenchymal stromal cells are killed by different pathways. Cytotherapy 2011;13:269–278.
58 Egea V, von Baumgarten L, Schichor C et al. TNF-alpha respecifies human mesenchymal stem cells to a neural fate and promotes migration toward experimental glioma. Cell Death Differ 18:853–863.
59 van Velthoven CT, Kavelaars A, van Bel F et al. Regeneration of the ischemic brain by engineered stem cells: Fuelling endogenous repair processes. Brain Res Rev 2009;61:1–13.
60 Takahashi K, Yamanaka S. Induction of pluripotent stem cells from mouse embryonic and adult fibroblast cultures by defined factors. Cell 2006;126:663–676.
61 Yu J, Vodyanik MA, Smuga-Otto K et al. Induced pluripotent stem cell lines derived from human somatic cells. Science 2007;318: 1917–1920.
62 Lowry WE, Richter L, Yachechko R et al. Generation of human induced pluripotent stem cells from dermal fibroblasts. Proc Natl Acad Sci USA 2008;105:2883–2888.
63 Hashimi ST, Fulcher JA, Chang MH et al. MicroRNA profiling identifies miR-34a and miR-21 and their target genes JAG1 and WNT1 in the coordinate regulation of dendritic cell differentiation. Blood 2009; 114:404–414.
64 Tarantino C, Paolella G, Cozzuto L et al. miRNA 34a, 100, and 137 modulate differentiation of mouse embryonic stem cells. FASEB J 2010;24:3255–3263.
65 Aranha MM, Santos DM, Xavier JM et al. Apoptosis-associated microRNAs are modulated in mouse, rat and human neural differentiation. BMC Genomics 2010;11:514.
66 Ikegami K, Ogyu S, Arakomo Y et al. Recovery of cognitive performance and fatigue after one night of sleep deprivation. J Occup Health 2009;51:412–422.
67 Condic ML, Rao M. Regulatory issues for personalized pluripotent cells. Stem Cells 2008;26:2753–2758.

See www.StemCells.com for supporting information available online.